High-Performance Robust Latches

Omana, M., Rossi, D. and Metra, M.

High Performance Robust Latches

Martin Omaña, Daniele Rossi, *Member*, *IEEE*, and Cecilia Metra, *Member, IEEE*

Abstract—First a new high performance robust latch (referred to as HiPeR latch) is presented, that is insensitive to transient faults affecting its internal and output nodes by design, independently of the size of its transistors. Then, a modified version of the HiPeR latch (referred as HiPeR-CG) is proposed, that is suitable to be used together with clock gating. Both proposed latches are faster than the latches most recently presented in the literature, while providing better or comparable robustness to transient faults, at comparable or lower costs in terms of area and power, respectively. Therefore, thanks to the good tradeoffs in terms of performance, robustness and cost, our proposed latches are particularly suitable to be adopted on critical paths.

Index Terms— Transient Faults, Soft Errors, Static Latch, Hardened Latch, Robust Design.

———————————————— ◆ ————————————————

1 INTRODUCTION

THE continuous advances of microelectronic technology are leading to an aggressive reduction of device dimensions down to the nanometer region. Because of the consequent reduction of circuit node capacitances, together with the simultaneous decrease of power supply voltages, the amount of charge stored on a circuit node is becoming increasingly smaller, making circuits more susceptible to spurious voltage glitches, caused by cosmic ray neutron or alpha-particle hits [1-5]. Such spurious voltage glitches are generally referred to as transient faults (TFs). If in the past TFs had been a concern only for space applications, nowadays they are recognized as a problem even at the sea level [6]. In particular, for terrestrial applications, high-energy neutrons are the dominating source of TFs, and the susceptibility of modern ICs to TFs is expected to increase with the scaling of technology node [7, 8, 9, 6].

When a TF affects a memory cell or a storage element (latch or flip-flop), it can cause a flip of the stored bit, thus giving rise to a soft error (SE), also referred to as single event upset (SEU). Soft errors have traditionally been recognized as a problem for high-density memories, because of their small cell size [10], [11]. Error correcting codes (ECCs), in particular single error correcting/double error detecting codes, have been successfully employed to guarantee a satisfactory level of memory reliability. Recently, because of the increasing probability of having multiple bit upsets [12], memory designers are facing new and challenging problems.

A SE may be also generated because of a TF affecting combinational logic, when the generated spurious voltage glitch propagates till the input of a sampling element. In this regard, however, it has been proven [13, 14] that SEUs affecting storage elements (latches and flip-flops) within sequential logic are by far the largest contributor to soft error rate (SER) in logic. For this reason, extensive research efforts have been recently devoted to devising novel hardening schemes/approaches for latches and flips-flops. Some approaches rely on the modifica-

tion of the latch structure in order to make it robust independently of the hitting particle energy. This is the case of the scheme proposed in [10], referred to as DICE cell, and the latch in [11, 15]. These latches make use of two independent feedback loops controlling the output. This way, a TF affecting one of the loops can not alter the output logic value. Also the latches in [13], [16] and [17] present this characteristic. As for the latches in [13, 16], their robustness relies on the deactivation of the feedback loop (during the latching phase), thus avoiding the generation of soft errors due to TFs affecting their nodes. The latch in [17], instead, re-uses the scan portion of a scan FF to duplicate the latch, thus producing two independent values, that are feeding an output stage first exploited in [18] for robust latches, then denoted as C-element in [17]. For all these latches, TFs affecting any of their internal or output nodes can not produce an output SE.

Other approaches aim at improving the latches' robustness against TFs by increasing node capacitances and/or the strength of some transistors. For instance, this approach is adopted by the latches in [19, 20, 21, 18, 22, 23]. In particular, the robustness of [19, 20, 21, 18] derives from the idea of either splitting the internal nodes and adopting proper feedback structures, or using a Schmitt trigger-like scheme. Instead, solutions in [22, 23] improve the latch robustness by inserting either explicit capacitances, or transistors acting as filters for voltage glitches. All latches in [19, 20, 21, 18, 22, 23] include nodes that, if affected by a TFs, may produce an output SE.

In this paper, first a new robust latch able to tolerate TFs independently of the hitting particle energy is presented. It is based on the latch structure introduced in [24], and will be hereinafter referred to as High Performance Robust (*HiPeR*) latch. Then, a modified version of such a *HiPeR* latch, referred to as *HiPeR-CG*, is also proposed, that is suitable to be used together with clock gating (*CG*) [25]. In fact, as shown in Section 4, TFs affecting some internal nodes of the *HiPeR* latch may leave its output in a high impedance state. If this event happens when clock gating is activated to reduce power consumption, the high impedance node may be improperly charged/discharged to an incorrect logic value due to leakage current, and a SE may originate. This is not expected to be a problem if clock gating is not adopted. In fact, also in the perspective of increasing leakage currents with technology scaling [26], since the latch operation

————————————————

• *M. Omaña, D. Rossi and C. Metra are with DEIS, Univ. of Bologna, Viale Risorgimento 2, 40136 Bologna, Italy, e-mail: {martin.omana, d.rossi, cecilia.metra}@unibo.it.*

frequency will also increase, the output of the latch will remain in a high impedance state for a time interval that will be too short to allow leakage currents to charge/discharge the output node.

To cope with the problem possibly arising in case of clock gating, the *HiPeR-CG* latch is proposed. Differently from *HiPeR*, *HiPeR-CG* is such that its output can not remain in a high impedance state when a TF affects any of its internal nodes, thus being suitable to be used together with clock gating.

The proposed latches are compared to each others, as well as to the standard latch [27], and to the most recently presented robust latches we are aware of [19, 13, 20, 15, 21, 16, 11]. The solution in [17] has not been considered for comparison purposes, since it is oriented to scan FFs.

It will be shown that the *HiPeR* and *HiPeR-CG* latches feature considerably better characteristics in terms of performance than all other considered robust latches, but for the latch in [20], which presents a comparable input-output delay. In addition, our proposed latches provide higher or comparable robustness to TFs compared to the considered alternative robust solutions, except for the latch in [15], which features the higher robustness. This latter, however, is the one with the highest cost in terms of area and power among all compared latches.

More in details, our latches feature higher area than the latches presenting lower robustness [19, 13, 20, 21, 16] while, as for power, the latch in [16] is the less consuming robust solution, but it is considerably slower and less robust than our proposed latches. Finally, compared to the latch in [11], the proposed solutions present comparable area, power and robustness, but are considerably faster. Therefore, thanks to the good tradeoffs in terms of performance, robustness and cost, our proposed latches are particularly suitable to be adopted on critical paths.

The rest of the paper is organized as follows. In Section 2, the *HiPeR* latch structure and behavior are described. In Section 3, some results of the electrical level simulations performed to verify the *HiPeR* latch behavior are reported. In Section 4, the effects of leakage currents on the *HiPeR* latch, when clock gating is applied, are analyzed. In Section 5, the *HiPeR-CG* latch is introduced. In Section 6, some results of the electrical level simulations performed to verify the *HiPeR-CG* latch behavior are reported. In Section 7, the proposed latches are compared to each others, and to alternative solutions (including the standard latch), considering cost and TF robustness as metrics for comparison. Finally, some conclusions are drawn in Section 8.

2   PROPOSED HIPER LATCH

The proposed *HiPeR* latch (Fig. 1) relies on two basic principles: i) triplication of the latch internal node driving a special output stage (first exploited in [18] for robust latches, then denoted as C-element in [17]) allowing the output to change its logic value accordingly to the value of the majority of the internal nodes; ii) design of two proper independent feedback loops, that are activated during the latching phase (here assumed to occur when CK=1).

The idea in i) above allows to tolerate TFs affecting internal nodes, while the design principle in ii) allows to tolerate also TFs affecting the output node. As for TFs affecting the input node, as discussed in details in Section 7, the *HiPeR* latch pro-

vides high robustness, similarly to the previous solutions in [13, 15, 16, 17, 11].

The electrical scheme of the proposed *HiPeR* latch is shown in Fig. 1. Transistors MN3 and MP4 (driven by the output Q) should be dominant over transistors MP3 and MN4 (driven by the internal node INT2), respectively. The behavior of the latch will be now described in details.

When CK=0, the latch is transparent, and the logic value *d* at the input node D propagates to the output Q and to the internal node *INT2* through transfer gates *TG1* and *TG2*, respectively. Then, the complemented logic value *d'* propagates to the internal nodes driving the output C-element, that is *INT3* (through inverter *I2*), *INT1a* (through the series *MP3-MN3*), and *INT1b* (through the series *MP4-MN4*). Thus, the C-element confirms the logic value *d* at the output node Q. It is worth noticing that, when CK=0, transistors *MP7* and *MN7* are OFF to avoid possible contention on node *INT2*. Furthermore, TFs affecting the latch during the clock low phase are not of concern, since the output of the latch is not valid during such a clock phase.

Instead, when CK=1, the transfer gates *TG1* and *TG2* are OFF and the input node *D* is disconnected from the output node *Q*. The value previously charged on node *Q* is maintained by the C-element, which is driven by two independent feedback loops (Fig. 1): i) the feedback loop denoted by *FL1*, including the output node *Q* and the internal nodes *INT1a* and *INT1b*; ii) the feedback loop denoted by *FL2*, composed by the back-to-back inverters *I1* and *I2* and including internal nodes *INT2* and *INT3*. This way, if a TF affects a latch internal node, it may change the state of only one of the two feedback loops, so that the logic value at the output *Q* is preserved. Furthermore, thanks to the previously mentioned dominance of transistors *MN3* and *MP4* (driven by the output *Q*) over transistors *MP3* and *MN4* (driven by internal node *INT2*), TFs affecting nodes *INT2* or *INT3* cannot change the logic values of nodes *INT1a* and *INT1b*, so that they cannot alter the output value *Q*.

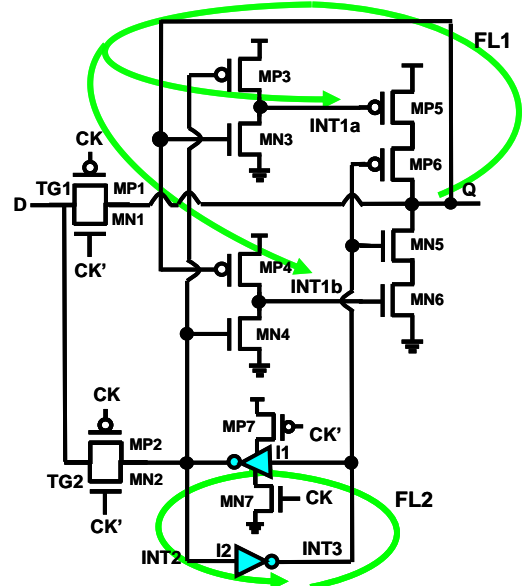Let us now describe in details the behavior of the latch in

Fig. 1. Electrical structure of the presented HiPeR latch.

case of TFs affecting its internal and output nodes when CK=1 (latching phase). In case of TFs affecting the internal node *INT1a*, the following two conditions can be distinguished: i) *Q*=1, thus *INT1a*=*INT3*=0 (the series *MP5-MP6* is on); ii) *Q*=0, thus *INT1a*=*INT3*=1 (the series *MP5-MP6* is OFF). In case i), the TF makes *INT1a* flip to 1, thus temporarily turning OFF *MP5*, and leaving the output *Q* in a high impedance state. However, the correct logic value of the output is not altered, and the conductive transistor *MN3* restores the correct value 0 on *INT1a*, thus making *MP5* turn on again. In case ii), the TF makes *INT1a* flip to 0, thus temporarily turning on *MP5*. However, since *INT3*=1, *MP6* is kept OFF and the logic value of *Q* is not altered.

Similarly, in case of TFs affecting *INT1b*, the following two conditions might be in order: i) *Q*=1, thus *INT1b*=*INT3*=0 (the series *MN5-MN6* is OFF); ii) *Q*=0, thus *INT1b*=*INT3*=1 (the series *MN5-MN6* is on). In case i), the TF makes *INT1b* flip to 1, thus temporarily turning *MN6* on. However, since *INT3*=0 (it is not altered by the TF) *MN5* remains OFF, and the logic value of *Q* is not altered. In case ii), the TF makes *INT1b* flip to 0, thus temporarily turning OFF *MN6* and leaving the output *Q* in a high impedance state, thus not altering its correct logic value.

As for TFs affecting *INT2* and *INT3*, they may produce incorrect logic values on both nodes *INT2* and *INT3*, since the positive feedback loop constituted by inverters *I1* and *I2* could confirm the wrong voltage value till the following CK cycle. The incorrect logic value on *INT2* may turn on transistors *MP3* or *MN4*, thus generating a contention between transistor *MP3* and *MN3* (that are driving node *INT1a*), or between transistors *MP4* and *MN4* (that are driving node *INT1b*). Despite the possible contention, *INT1a* and *INT1b* do not change their logic value, since *MN3* and *MP4* (driven by the output node *Q*) are dominant over *MP3* and *MN4*. However, the electrical conflict gives rise to an increase in static power consumption till the following clock cycle. Moreover, both the series *MP5-MP6* and *MN5-MN6* are turned OFF, thus leaving node *Q* in a high impedance state, so that the correct output value is maintained and the latch keeps on working correctly.

As for TFs affecting the output node *Q* when CK=1, similarly to the case of the previous solutions in [11, 13], they generate only a voltage glitch, whose width and amplitude depend directly on the amount of charge injected by the hitting particle, and inversely on the strength of the transistor driving the node (that is, the series *MP5-MP6* or *MN5-MN6*) and on the fan-out load. Afterwards, since the series of transistors driving the output node keeps on conducting also after the TF exhaustion, the correct output value is restored.

Finally, let us consider the case of a TF affecting node *INT2* or *INT3* when the clock is gated. If a following TF affects node *Q*, an incorrect logic value may be feedbacked, thus giving rise to a SE. However, the likelihood of this event (that is the combination of a TF affecting *INT2* or *INT3*, followed by a second TF affecting node *Q*) can be considered negligible, especially for latches adopted for terrestrial applications.

3 HIPER LATCH IMPLEMENTATION AND VERIFICATION

The proposed *HiPeR* latch has been implemented considering a standard 90nm CMOS technology with $V_{dd} = 1V$ and a clock frequency of 500MHz. The transistors have the following aspect ratios (Fig. 1): (i) *(W/L) = 1* for the transistors *MN2, MN3, MN4, MN5, MN6, MN7, MP3,* and the nMOS of inverters *I1* and *I2*; (ii) *(W/L) = 2* for the transistors *MN1, MP2, MP5, MP6, MP7* and the pMOS of inverters *I1* and *I2*; (iii) *(W/L) = 4* for the transistors *MP1* and *MP4*. As for the clock signal, it has been generated by a buffer with a conductance equal to 10x that of a minimum sized symmetric inverter.

The behavior of the *HiPeR* latch qualitatively described in the previous section has been verified by means of conventional and Monte Carlo electrical level simulations, performed considering statistical variations (with uniform distribution) up to the 20% of power supply, oxide thickness, transistor threshold voltage, and electron/hole mobility.

Transient faults producing both negative glitches (on nodes with a high logic value) and positive glitches (on nodes with a low logic value) have been emulated by connecting to the affected node an ideal current generator, denoted by $I_{inj}(t)$. As proposed in [1], and reported in Eq. (1), it presents a double exponential pulse shape current, allowing to emulate the current produced by an alpha-particle hit

$$I_{inj}(t) = I_0 \left(e^{-t/\tau_\alpha} - e^{-t/\tau_\beta} \right) \tag{1}$$

The parameter I_0 depends on the amount of injected charge, while τ_α represents the collection time-constant of the junction, and τ_β accounts for the ion-track establishment time constant [28].

As an example, Figures 2-4 report the results of some simulations performed during the latching phase (i.e., when CK=1), under nominal values of electrical parameters. Particularly, Figs. 2(a) and (b) show the effects of TFs affecting the internal nodes *INT1a* and *INT1b*, respectively. As can be seen, the particle hits produce a voltage glitch that changes temporarily the logical state of the affected node. However, as described before, the correct logic value of *INT1a* and *INT1b* are restored by the respective driving transistors, so that the logic value of the output Q is not altered by these TFs.

Similarly, Figs. 3(a) and (b) report the effects of TFs affecting the internal nodes *INT2* and *INT3*, respectively. The particle hits make the logic values of both nodes *INT2* and *INT3* flip. Although these incorrect logic values are maintained till the following falling edge of CK, the correct logic value of the output Q is not altered, and the latch keeps on working correctly.
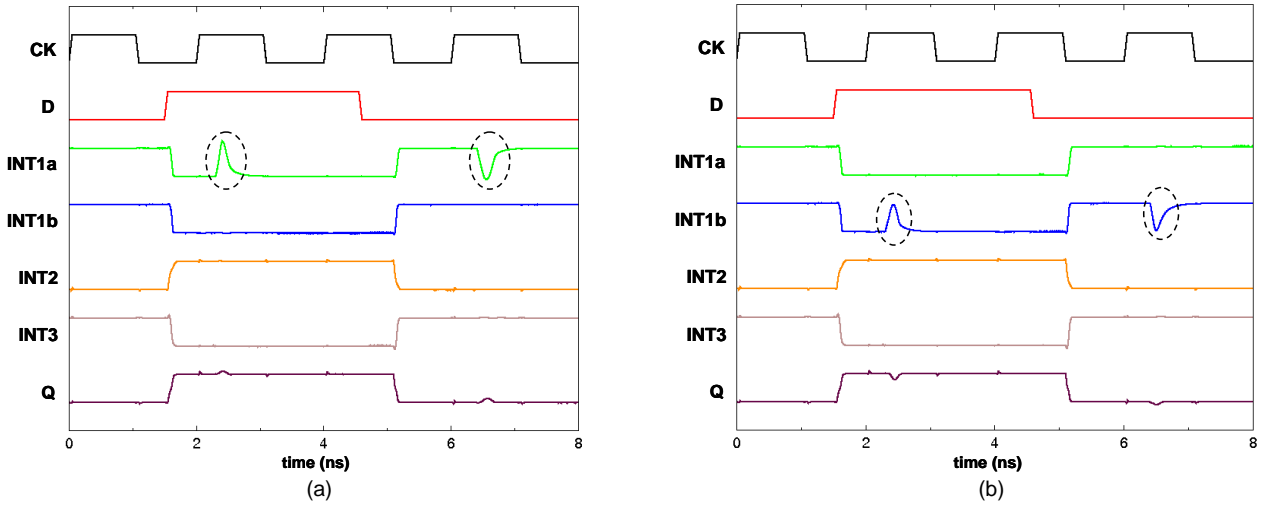
Fig. 2. Simulation results obtained for nominal values of electrical parameters and TFs affecting the internal feedback nodes INT1a (a) and INT1b (b).
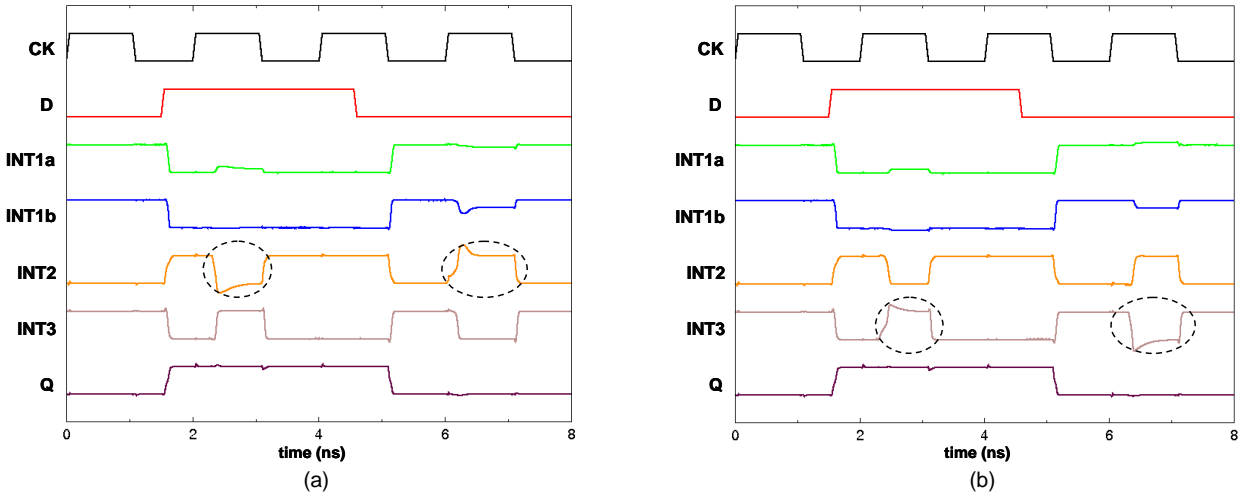

Fig. 3. Simulation results obtained for nominal values of electrical parameters and TFs affecting the internal feedback nodes INT2 (a) and INT3 (b).
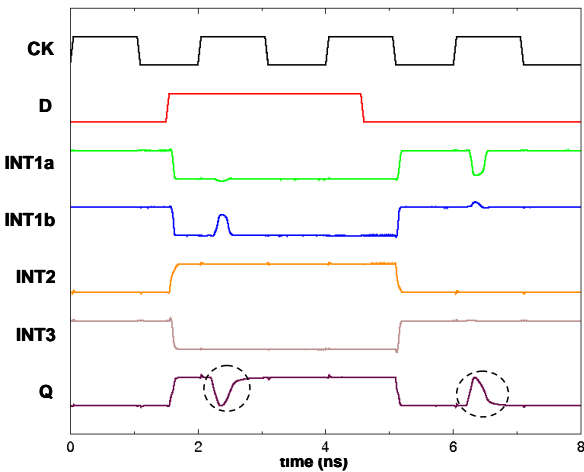

Fig. 4. Simulation results obtained for nominal values of electrical parameters and TFs affecting the output node Q.

Finally, Fig. 4 shows the effects of TFs affecting the latch output node *Q*. The particle hits produce a voltage glitch on the output node, that changes temporarily its logical state. The correct output logic value is recovered within a time interval that depends directly on the amount of charge injected by the hitting particle, and inversely on the conductance of the transistors driving the output node (i.e., the series *MP5-MP6* and *MN5-MN6*). It is worth noticing that, even though the correct value of *Q* is restored, the glitch generated at the output *Q* may propagate through the downstream logic and be captured by a memory element, or it may alter the value stored in a high impedance node within a dynamic circuit, thus possibly resulting in a SE. However, this may be the case also for all robust latches. This will be taken into account in the evaluation of the robustness of the compared latches in Section 7.

Results analogous to those shown in Figs. 2-4 have been obtained also by means of Monte Carlo simulations accounting for electrical parameter variations, as clarified at the beginning of this section.

4 EFFECTS OF LEAKAGE CURRENTS ON THE HIPER LATCH

In this section, we analyze the effects that leakage currents can produce on the *HiPeR* latch, when clock gating is employed to reduce power consumption.

As described in Section 2, TFs affecting nodes *INT2* or *INT3* when CK=1 may produce incorrect logic values on both nodes *INT2* and *INT3*. These incorrect logic values are maintained till the next clock phase making the latch transparent (CK=0). As a consequence, a contention between transistors *MP3* and *MN3* (driving node *INT1a*), or between transistors *MP4* and *MN4* (driving node *INT1b*) is generated. This contention does not change the logic values on *INT1a* and *INT1b*, thanks to the dominance of transistors *MN3* and *MP4* over transistors *MP3* and *MN4*, respectively. However, it gives rise to static power consumption. Moreover, the flip of *INT2* and *INT3* moves one of the internal nodes *INT1a* (if *Q*=0), or *INT1b* (if *Q*=1) to a high impedance state. In addition, the output C-element is turned OFF, thus making the output node *Q* be also in a high impedance state till the next clock low phase, thus retaining its correct logic value.

As introduced earlier, even in the perspective of significantly increased leakage currents with scaled technologies, since the latch operation frequency will also increase with scaling, the output *Q* and nodes *INT1a* or *INT1b* will remain in a high im-

pedance state for a time interval lower or equal to half clock cycle, which will not be long enough to allow also high leakage currents to change the logic value of these nodes.

Instead, if clock gating is implemented to reduce power consumption, the clock may be fixed to a constant value for long time intervals, which can be much longer than a single clock period. In this case, if a TF affects either *INT2* or *INT3*, nodes *Q* and *INT1a*, or *INT1b* may remain in a high impedance state for a time interval long enough to be possibly charged/discharged to incorrect logic values by leakage currents.

In order to analyze in details the effects of TFs affecting *INT2* or *INT3* when clock gating is activated, electrical level simulations have been performed, considering the same technology, power supply and implementation of the *HiPeR* latch reported in the previous section. The obtained results are shown in Figs. 5(a), (b), (c) and (d).

Particularly, Fig. 5(a) shows the case of a TF occurring at time t_1 and affecting node *INT2* when it presents a low logic value, while Fig. 5(b) reports the case of a TF affecting *INT2* when it is at a high logic value. Similarly, the cases of TFs affecting node *INT3* when it presents a low and a high logic value are shown in Figs. 5(c) and (d), respectively.

It can be observed that, in all cases, after the particle hit, nodes *INT2* and *INT3* flip to an incorrect logic value, thus turning off the output C-element and leaving the output *Q* in a high impedance state. Particularly, after the particle hit (at time t_1), the voltage on the output node *Q* starts slowly swinging to an

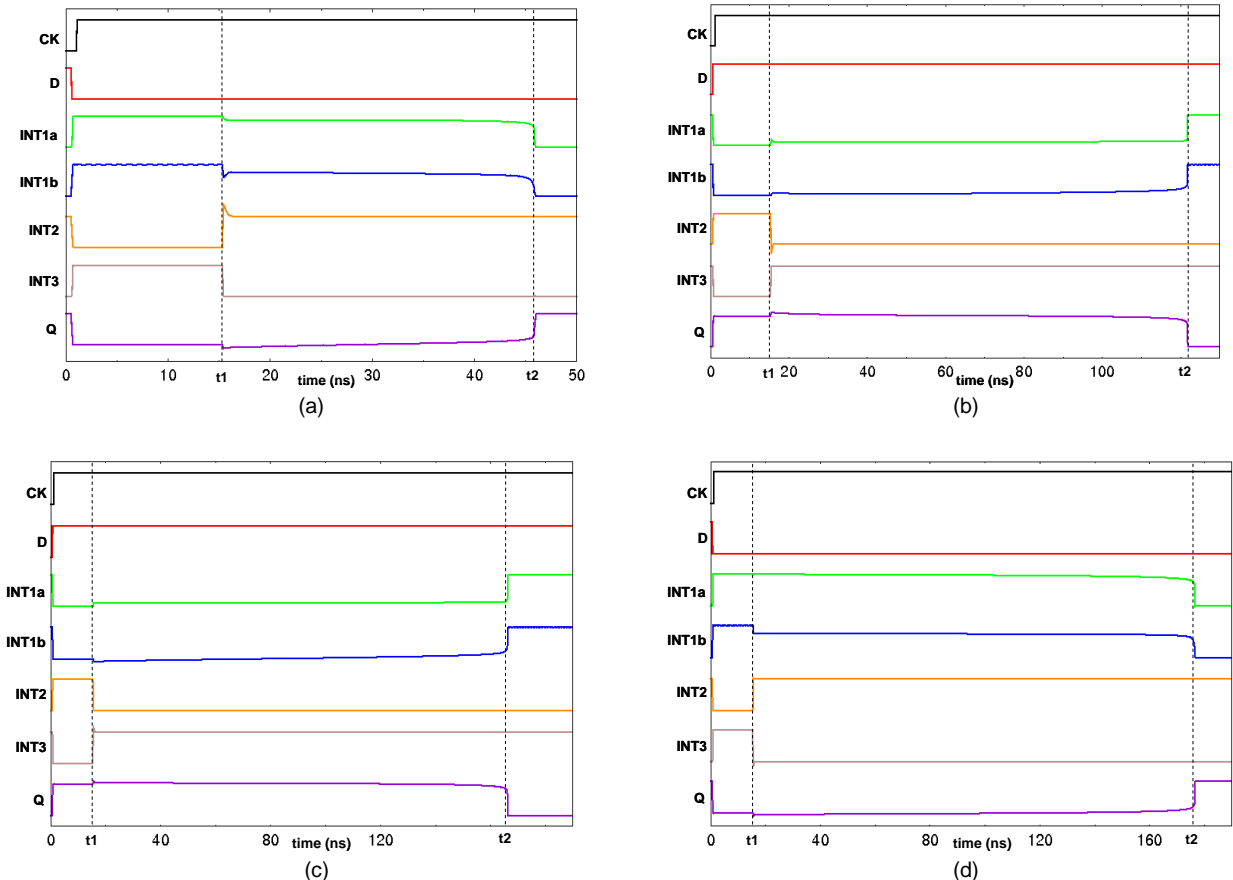
Fig. 5. Simulation results for the HiPeR latch when the clock is kept constant to a high logic value and (a) a TF affects INT2 at t1, when it presents a low logic value; (b) a TF affects INT2 at t1, when it presents a high logic value; (c) a TF affects INT3 at t1, when it presents a low logic value; (d) a TF affects INT3 at t1, when it presents a high logic value.

incorrect logic value due to leakage currents. After a time interval $\Delta t = t_2 - t_1$ ranging from 31ns (Fig. 5(a)) to 149ns (Fig. 5(d)), the output node Q moves to an incorrect logic value.

More in details, from Figs 5(a) and (d) it can be observed how leakage currents flowing through the series $MP5$-$MP6$ and $MN5$-$MN6$ start to slightly charge the node Q after t_1, while from Figs 5(b) and (c) we can observe how such leakage currents start to slightly discharge the node Q after t_1. This process continues during the time interval $\Delta t = t_2 - t_1$ (Figs 5(a), (b), (c) and (d)). As described before, during Δt an incorrect logic value of $INT2$ (i.e., provoked by a TF affecting $INT2$ or $INT3$) may turn on transistors $MP3$ or $MN4$ (Fig. 1), thus generating a contention between transistors $MP3$ and $MN3$ (which drive node $INT1a$), or between transistors $MP4$ and $MN4$ (which drive node $INT1b$). The logic value on nodes $INT1a$ and $INT1b$ is not changed by this contention, because $MN3$ and $MP4$ are designed to be dominant over $MP3$ and $MN4$. However, the continuous increase (decrease) of the voltage on node Q due to leakage makes transistor $MP4$ (if Q=0, in Figs. 5(a), (d)) or $MN3$ (if Q=1, in Figs. 5(b), (c)) become less conductive, thus less dominant over transistor $MN4$ or $MP3$, respectively. At time t_2, transistors $MP4$ or $MN3$ are eventually no longer dominant over $MN4$ or $MP3$, and nodes $INT1a$ and $INT1b$ flip to an incorrect logic value, thus making the latch provide a wrong output value.

5 PROPOSED HIPER-CG LATCH

In order to avoid the problems described in the previous section, which might originate if clock gating is adopted, a simple modification to the $HiPeR$ latch is here proposed. This solution, hereinafter referred to as $HiPeR$-CG, is suitable to be used together with clock gating. In fact, it prevents the output Q from being in a high impedance state, after a TF affects any of its internal nodes. The electrical scheme of such a proposed latch is shown in Fig. 6.

The main differences with respect to the $HiPeR$ latch are the following: i) the pMOS transistor $MP7$ is now driven by the internal node $INT1a$, rather than by CK'; ii) the nMOS transistor $MN7$ is now driven by the internal node $INT1b$, rather than by CK; iii) addition of two transistors $MP8$ and $MN8$ driven by the output node Q; iv) addition of the transistor $MN10$, driven by CK, in series with $MN5$ and $MN6$, thus modifying the output C-element.

Let us now describe the behavior of the $HiPeR$-CG latch.

When CK=0, the logic value (d) present at the input node D propagates to the output Q through transfer gate $TG1$, and to $INT2$ through transfer gate $TG2$. Since the voltage on Q is equal to the voltage on $INT2$, the complemented logic value of the input is propagated to $INT3$ (through the C-element composed by $MP8$, $MN8$ and $I2$) and to $INT1a$ (through $MP3$ or $MN3$, depending on whether d=0 or d=1, respectively) and to $INT1b$ (through $MP4$ or $MN4$, depending on whether d=0 or d=1, respectively). Thus, $INT1a$=$INT1b$=$INT3$, and the logic value on $INT2$ is confirmed by the C-element composed by $MP7$, $MN7$ and $I1$. It is worth noticing that, when CK=0, the additional transistor $MN10$ is OFF, thus avoiding possible contentions between the gate driving the latch input and the series transistors $MN10$-$MN5$-$MN6$.

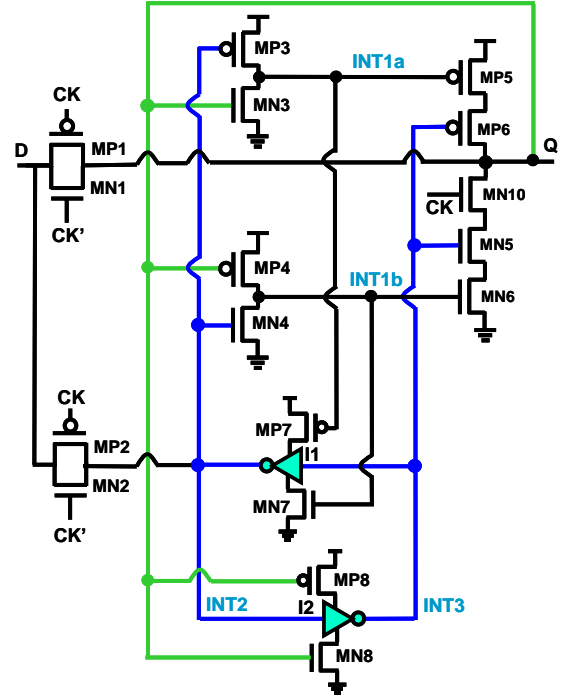Instead, when CK=1, transfer gates $TG1$ and $TG2$ are turned

Fig. 6. Electrical structure of the proposed HiPeR-CG latch.

off, while transistor $MN10$ is turned on. As a consequence, the value previously present on node Q is maintained by the modified output C-element.

The behavior of the proposed $HiPeR$-CG latch in case of TFs is similar to that of the latch in Fig. 1, described in Section 2. However, node $INT2$ is now driven by a C-element composed by the transistors $MP7$ and $MN7$ and the inverter I1, thus avoiding that TFs generated on node $INT3$ can propagate to $INT2$. Similarly, node $INT3$ is driven by another C-element composed by the transistors $MP8$ and $MN8$ and the inverter $I2$, thus preventing TFs generated on node $INT2$ from being propagated to $INT3$. Therefore, differently from the $HiPeR$ latch, TFs affecting nodes $INT2$ or $INT3$ of the $HiPeR$-CG latch produce a voltage glitch that is not confirmed, so that the correct voltage value is recovered on the hit node (i.e., $INT2$ or $INT3$), and the output node Q is not left in a high impedance state.

Finally, as for TFs affecting the other latch nodes (i.e., nodes $INT1a$, $INT1b$, and Q), similarly to the case of the $HiPeR$ latch, they are tolerated.

6 HIPER-CG LATCH IMPLEMENTATION AND VERIFICATION

The $HiPeR$-CG latch has been implemented considering a standard 90nm CMOS technology with V_{dd} = 1V. The following transistor aspect ratios have been considered (Fig. 6): (i) (W/L)=1 for the transistors $MN2$, $MN3$, $MN4$, $MN5$, $MN6$, $MN7$, $MN8$, $MN10$, $MP3$ and the nMOS of inverters I1 and $I2$; (ii) (W/L)=2 for the transistors $MN1$, $MP2$, $MP5$, $MP6$, $MP7$, $MP8$ and the pMOS of inverters I1 and $I2$; (iii) (W/L)=4 for the transistors $MP1$ and $MP4$. The particle hits have been emulated by connecting an ideal current generator to the affected node, as described in Section 3.

As for the *HiPeR-CG* latch behavior, considerations analogous to those given for the *HiPeR* latch hold true in case of normal operation (that is, without clock gating). Instead, when clock gating is applied, the *HiPeR-CG* latch differs considerably from the *HiPeR* latch. The simulation results achieved for this latter case are here reported.

Figs. 7(a), (b), (c) and (d) show the cases of TFs affecting either *INT2* or *INT3* at a time instant denoted by t_1, while keeping the clock fixed at its latching value (CK = 1 in our case) for long time intervals.

More in details, Fig. 7(a) and (b) report the cases of a TF affecting node *INT2* when it presents a low and a high logic value, respectively. As can be seen, the particle hits produce a voltage glitch that changes temporarily the state of the affected node. However, the correct logic values of *INT2* and *INT3* are restored after a time interval depending on the particle energy, strength of the transistors driving the node and node capacitance.

Analogous considerations hold true for the case of TFs affecting *INT3*, reported in Figs. 7(c) and (d). However, the logic value of the output *Q* is not altered by these TFs in all considered cases.

7   COMPARISON EITH ALTERNATIVE SOLUTIONS

In this section, the proposed *HiPeR* (Fig. 1) and *HiPeR-CG* latches (Fig. 6) are compared with the standard latch [27] and with the most recently proposed robust latches in [19, 13, 20, 15, 21, 16, 11], considering robustness against TFs and cost (in terms of area, power and delay). The solution in [17] has not been considered for comparison purposes, since it has been proposed for scan FFs.

Electrical level simulations of all compared latches have been performed employing a standard 90nm CMOS technology, V_{dd} = 1V and a clock frequency of 500MHz. Additionally, for the purpose of comparison, the case of minimal area design (i.e., minimum possible transistor sizes making the latches work properly) has been considered for all latches.

7.1 Robustness Against TFs

In this subsection, the robustness of the considered latches against TFs are evaluated and compared to each other. As discussed in [20], the SER of a latch can be expressed by the sum of several contributions, each referred to a node of the latch. In turn, the TF susceptibility of each node can be expressed as a function of: i) the window-of-vulnerability (WOV), which is the time interval within a CK period (T_{CK}) during which a TF hitting the node can propagate till the output of the latch and give rise to a SE; ii) the critical charge (Q_{crit}) of the considered node, that is the amount of charge collected by the hit node that produces a voltage glitch with an amplitude exceeding the logic threshold of the fan-out gate. Therefore, the total SER for a latch is given by:

$$SER = \sum_{i=1}^{n} \frac{WOV_i}{T_{CK}} \cdot \kappa_i \cdot \alpha \cdot e^{-\beta \cdot Q_{crit}(i)} \qquad (2)$$
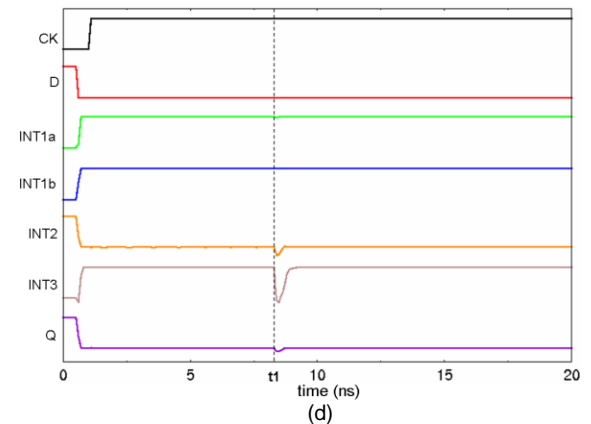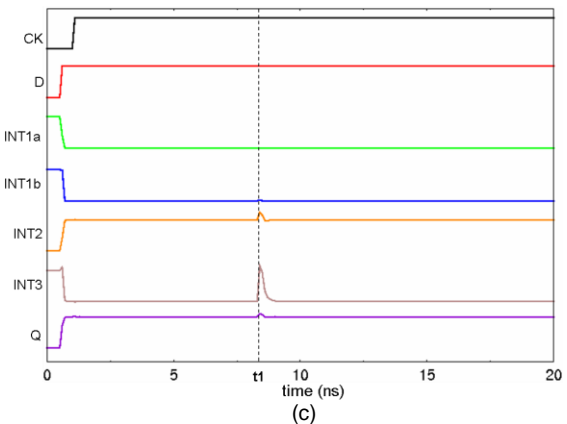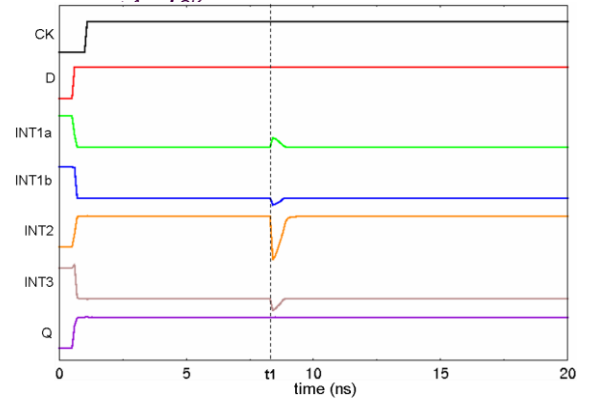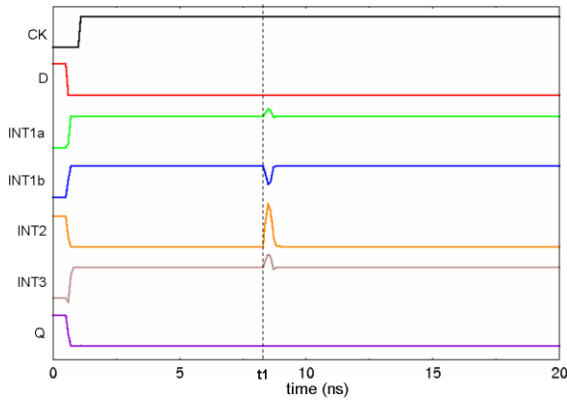

Fig. 7. Simulation results for the HiPeR-CG latch when the clock is kept constant to a high logic value and (a) a TF affects INT2 at t1, when it presents a low logic value; (b) a TF affects INT2 at t1, when it presents a high logic value; (c) a TF affects INT3 at t1, when it presents a low logic value; (d) a TF affects INT3 at t1, when it presents a high logic value.

where n is the number of nodes, κ_i is a constant proportional to the area of the node i, and α and β are fitting parameters.

As discussed in [20], SEs caused by TFs affecting the internal/output nodes of a latch are the major contributors to the overall latch SER, while SEs caused by TFs affecting the latch input node have a marginal impact. This mainly because the WOV of the latch input node (which is generally equal to the latch setup time) is considerably smaller than the WOVs of the latch internal and output nodes, which is generally equal to half of the CK period [20], that is to the clock latching phase (CK = 1 for all considered latches). Therefore, for comparison purposes, the robustness of the latches has been evaluated by considering only TFs affecting their internal and output nodes when CK=1.

In order to compare the robustness of the latches, the critical charges of internal and output nodes for all considered latches are evaluated. We can distinguish three kinds of nodes. Nodes of kind i), that is nodes such that an affecting TF produces only a voltage glitch on the node, without propagating to (i.e., affecting) the output node Q, independently of the energy of the hitting particle. For these nodes, the critical charge is conventionally set to infinity: $Q_{crit} \rightarrow \infty$. Nodes of kind ii), that is nodes such that an affecting TF produces a voltage glitch that may propagate to the output Q, whose correct value is restored after a time interval depending on the particle energy, on the strength of the transistor driving the node and on the node capacitance. As discussed previously, even though the correct value of Q is restored, the glitch generated at the output may propagate through the downstream logic and be captured by a memory element, or it may alter the value stored in a high impedance node within a dynamic circuit, thus possibly producing a SE. For such nodes, the critical charge Q_{crit} is evaluated by means of Hspice simulations, as the amount of collected charge that generates an output glitch with an amplitude equal to half the power supply, that is equal to the logic threshold of a symmetric fan-out gate. Finally we can identify nodes of kind iii), namely nodes such that an affecting TF produces an upset at the output of the latch. This is the most critical kind of nodes, since an output soft error may be generated. Analogously to nodes of kind ii), the critical charge Q_{crit} is evaluated by measuring (by means of Hspice) the amount of collected charge resulting in an output voltage glitch equal to the fan-out logic threshold.

As for the proposed *HiPeR* latch, TFs affecting the internal nodes *INT1a* and *INT1b* do not alter the logic value of the output Q (they are tolerated by design). Therefore, these nodes are of kind i) and their critical charge is assumed to be $Q_{crit(INT1a)} = Q_{crit(INT1b)} \rightarrow \infty$. Analogous considerations hold true for nodes *INT2* and *INT3*, so that $Q_{crit(INT2)} = Q_{crit(INT3)} \rightarrow \infty$. As for TFs affecting directly the output node Q, they produce a voltage glitch on such a node that is recovered after a time interval depending on the particle energy, on the strength of the transistor driving the node and on the node capacitance. Therefore, this node is a node of kind ii) and, from Hspice simulations, a critical charge $Q_{crit(Q)} = 7fC$ has been estimated. Finally, considering the *HiPeR-CG* latch, results analogous to those obtained for the

HiPeR latch have been found. Particularly, it is $Q_{crit(Q)} = 7.9fC$.

In order to compare the robustness of all considered latches, two metrics are introduced. They are denoted by R_{HiPeR} and $R_{HiPeR-CG}$, and report the ratios between the SER of the compared latches and that of the HiPeR and HiPeR-CG latch, respectively. They are defined as follows:

$$R_{HiPeR}(comp\_latches) = \frac{SER(comp\_latches)}{SER(HiPeR)} = \frac{\sum_{i=1}^{n} P_{Ni}\cdot\alpha\cdot e^{-\beta\cdot Qcrit(i)}\Big|_{comp\_latches}}{\sum_{j=1}^{n} P_{Nj}\cdot\alpha\cdot e^{-\beta\cdot Qcrit(j)}\Big|_{HiPeR}} \quad (3)$$

$$R_{HiPeR-CG}(comp\_latches) = \frac{SER(comp\_latches)}{SER(HiPeR-CG)} = \frac{\sum_{i=1}^{n} P_{Ni}\cdot\alpha\cdot e^{-\beta\cdot Qcrit(i)}\Big|_{comp\_latches}}{\sum_{j=1}^{n} P_{Nj}\cdot\alpha\cdot e^{-\beta\cdot Qcrit(j)}\Big|_{HiPeR-CG}} \quad (4)$$

If R>1, the reference latch (HiPeR or HiPeR-CG) is more robust against TFs than the compared latch. The factor P_{Ni} (proportional to parameter κ_i in (2)) accounts for the probability that a TF affecting the circuit hits a susceptible node. It is given by:

$$P_{Ni} = \frac{A_{Di}}{A_{TOT}} \quad (5)$$

where A_{Di} represents the (susceptible) area of the drain junctions of node i, while A_{TOT} represents the area of all compared latches (employed as a normalization factor). For the HiPeR and HiPeR-CG latches, the following values of P_{Ni} have been found: $P_{INT1a}= 0.007$; $P_{INT1b} = 0.018$; $P_{INT2}= 0.021$; $P_{INT3}= 0.011$; $P_Q= 0.032$.

Evaluations analogous to those carried out for the proposed latches have been performed also for all compared latches. The obtained results are summarized in Tab. 1. For each latch, the table reports the number of susceptible nodes and their kind, the total susceptible area normalized to the total area of the latches, considering only nodes of kind ii) and iii), and the minimum and maximum values of the critical charge obtained considering all susceptible nodes. Finally, the last two columns report the values of the estimated R_{HiPeR} and $R_{HiPeR-CG}$, as defined in (3) and (4), respectively, whose values have been computed deriving the value of the parameter β from [29] ($\beta = 72 \times 10^{12}$ $1/C$ for the considered 90nm CMOS technology).

As can be seen, the standard latch, as well as the robust latches in [19, 20, 21] include nodes of kind iii), so that a TF affecting these nodes may result in a soft error. Instead, all other latches, including the proposed ones, present only nodes of kind i) and ii), thus avoiding the generation of a SE at the latch output. Among all robust latches, the HiPeR and HiPeR-CG feature higher or comparable robustness, but for the latch in [15]. However, as clarified in the following subsection, this latter requires higher area overhead, propagation delay and power consumption.

7.2 Cost Comparison

The cost of the latches has been compared in terms of required area overhead, propagation delay, power consumption and power-delay product. Electrical level simulations of all compared latches have been performed, considering a standard 90nm CMOS technology, $V_{dd} = 1V$ and a clock frequency of 500MHz. The propagation delay has been estimated by evaluating the input-output delay (τ_{D-Q}) when the latch is transparent. Particularly, it has been obtained by averaging the time elapsing between the occurrence of a transition at the latch input and the occurrence of the corresponding transition of the latch output (both measured at the 50% of V_{dd}) for both 0➔1 and 1➔0 input transitions. Finally, as for power consumption, it has been evaluated assuming an input switching activity of 25%. Moreover, the power consumption of the clock drivers has been included in the evaluation. For all latches, a clock driver composed by two cascaded inverters with aspect ratios $(W/L)_P=20$ and $(W/L)_N=10$ has been considered. The static power consumption due to leakage has been included as well.

The results of the performed evaluations are reported in Tab. 2. As can be seen, apart from the standard latch, the robust latches in [21, 13] are the smallest, while the proposed *HiPeR-CG* latch is the one with the highest performance. The latch in [16] is the one with the lowest power, and power delay product.

For a detailed comparison, the relative cost in terms of area (ΔA), power consumption (ΔP), propagation delay (Δd) and power-delay product ($\Delta(P \times d)$) of the considered latches over the *HiPeR* and *HiPeR-CG* latches are reported in Tab. 3. In the last column, the relative SER (ΔSER) is also reported. For the *HiPeR* latch, the relative variations have been computed as: $\Delta = 100 \cdot (HiPeR - compared\_latch) / HiPeR)$. Similarly, for the *HiPeR-CG* latch.

Compared to the standard latch, similarly to all considered robust solutions, our latches require higher area overhead and power consumption.

As for propagation delay, our proposed latches are faster than all other considered latches (included the standard one).

TABLE 1
COMPARISON OF THE ROBUSTNESS OF THE HIPER LATCH ($R_{SER-HIPER}$) AND THE HIPER-CG LATCH ($R_{SER-HIPER-CG}$) WITH THAT OF THE STANDARD LATCH AND THE OTHER CONSIDERED ROBUST LATCHES

	Number of susceptible nodes	Normalized susceptible area (class ii and iii)	Qcrit (fC) min	Qcrit (fC) max	$R_{SER\text{-}HiPeR}$	$R_{SER\text{-}HiPeR\text{-}CG}$
HiPeR	4 of kind i) 1 of kind ii)	0.032	7	→+∞	-	1.06
HiPeR-CG	4 of kind i) 1 of kind ii)	0.032	7.9	→+∞	0.94	-
Standard	3 of kind iii)	0.074	6	10.6	2.09	2.23
Latch in [11]	2 of kind i) 3 of kind ii)	0.085	20	→+∞	0.97	1.03
Latch in [16]	4 of kind i) 3 of kind ii)	0.032	4.6	→+∞	1.04	1.1
Latch in [21]	3 of kind iii)	0.085	8.5	29.6	1.77	1.87
Latch in [15]	3 of kind i) 2 of kind ii)	0.042	9.1	→+∞	0.89	0.95
Latch in [20]	2 of kind i) 1 of kind ii)	0.042	8.7	→+∞	1.18	1.26
Latch in [13]	2 of kind i) 3 of kind ii)	0.074	12.5	→+∞	1.1	1.17
Latch in [19]	2 of kind i) 3 of kind iii)	0.106	8.1	→+∞	1.59	1.69

TABLE 2
ABSOLUTE COST OF THE COMPARED LATCHES

	Area (Sq)	Prop. delay (ps)	Power (µW)	Power × delay (au)
HiPeR	31	60.8	1.4	85.2
HiPeR-CG	35	**57.1**	1.6	91.4
Standard	**18**	73.7	**0.64**	**47.2**
Latch in [11]	32	76.7	1.58	121.2
Latch in [16]	27	81.5	0.79	64.4
Latch in [21]	21	168.5	1.73	291.5
Latch in [15]	48	114.5	3.03	346.9
Latch in [20]	24	59.2	1.3	76.9
Latch in [13]	21	71.2	0.87	61.9
Latch in [19]	27	81.2	1.39	112.8

TABLE 3
RELATIVE COST AND ROBUSTNESS OF THE COMPARED LATCHES WITH RESPECT TO THOSE OF THE HIPER LATCH (FIG. 1) AND THE HIPER-CG LATCH (FIG. 6)

Latch	HiPeR ΔA	Δd	ΔP	Δ(P×d)	ΔSER	HiPeR-CG ΔA	Δd	ΔP	Δ(P×d)	ΔSER
HiPeR	-	-	-	-	-	-11.4%	+6.5%	-12.5%	-6.8%	+6.3%
HiPeR-CG	+12.9%	-6.1%	+14.3%	+7.3%	-6%	-	-	-	-	-
Standard	-41.9%	+21.1%	-54.3%	-44.6%	+109%	-48.6%	+29%	-60%	-48.4%	+122%
Latch in [11]	+3.2%	+26%	+12.9%	+42.3%	-3%	-8.6%	+34.2%	-1.3%	+32.5%	+3.2%
Latch in [16]	-12.9%	+34%	-43.6%	-24.4%	+3.8%	-22.8%	+42.7%	-50.6%	-29.5%	+10.4%
Latch in [21]	-32.2%	+177%	+23.6%	+242%	+77.3%	-40%	+195%	+8.1%	+219%	+88.6%
Latch in [15]	+54%	+88.2%	+116%	+307%	-10.5%	+37%	+100%	+89.4%	+279%	-4.8%
Latch in [20]	-22.6%	-2.8%	-7.1%	-9.7%	+18.4%	-31.4%	+3.5%	-18.8%	-15.9%	+25.9%
Latch in [13]	-32.3%	+39%	-37.9%	-27.3%	+10.2%	-40%	+24.6%	-45.6%	-32.3%	+17.2%
Latch in [19]	-12.9	+33.4%	+0.7%	+32.5%	+59%	-22.8%	+42.1%	-13.1%	+23.4%	+69.1%

Particularly, the *HiPeR-CG* latch is the fastest one, with a propagation delay slightly lower (-6%) than that of the *HiPeR* latch. Compared to the *HiPeR-CG* latch, the increase in propagation delay of the alternative solutions ranges from +3.4% for the latch in [20], to +195% for the latch in [21].

As for robustness, the *HiPeR* and *HiPeR-CG* latches feature a SER that is lower than, or comparable to that of the other considered latches, but for the latch in [15], which features a lower SER, but requires a higher area overhead, propagation delay and power consumption.

As for area overhead, our latches feature higher area than the latches in [19, 13, 20, 21, 16] which, however, are considerably slower and provide a higher SER.

As for power consumption, the *HiPeR* and *HiPeR-CG* latches consume more power than the scheme in [16, 20, 13, 19] which, however, are slower and less robust.

8 CONCLUSIONS

In this paper first a new high performance robust latch (denoted as *HiPeR* latch) has been presented. It is insensitive to TFs affecting its internal and output nodes by design, independently of the energy of the hitting particles. Then, a modified version of the *HiPeR* latch (denoted as *HiPeR-CG* latch) has been proposed, that is suitable to be used together with clock gating. In fact, as shown in the paper, when clock gating is implemented to reduce power consumption, TFs affecting some internal nodes of the *HiPeR* latch may leave its output

node in a high impedance state, thus possibly allowing leakage currents to change the stored logic value, with consequent reliability risks. It has been shown that this problem is overcome by the proposed *HiPeR-CG* latch at the cost of 13% extra area, and with no impact on performance, which is indeed improved.

It has been shown that the *HiPeR* and *HiPeR-CG* latches feature considerably better characteristics in terms of performance compared to all other considered robust latches, but for the latch in [20], which presents comparable input-output delay, but features a considerably lower robustness to TFs. In addition, our proposed latches provide higher or comparable robustness to TFs compared to the considered alternative robust solutions, except for the latch in [15], which features the higher robustness, but requires higher costs in terms of area and power.

More in details, our latches features higher area than the latches presenting lower robustness [19, 13, 20, 21, 16]. As for power, the latch in [16] is the less consuming, but it is considerably slower and less robust than our proposed latches. Finally, compared to the latch in [11], the proposed solutions present comparable area, power and robustness, but are considerably faster. Therefore, thanks to the good tradeoffs in terms of performance, robustness and cost, our proposed latches are particularly suitable to be adopted on critical paths.

REFERENCES

[1] G. C. Messenger, "Collection of Charge on Junction Nodes from Ion Tracks", *IEEE Trans. on Nuclear Science*, NS-29(6), pp. 2024 - 2031, December 1982.

[2] C. M. Hsieh, P. C. Murley, R. R. O'Brien, "Collection of Charge from Alpha-Particle Tracks in Silicon Devices", *IEEE Trans. on Electron Devices*, ED-30, pp. 686 - 693, 1983.

[3] S. Kang, D. Chu, "CMOS Circuit Design for the Prevention of Single Event Upset", in *Proc. of IEEE Int. Conf. on Computer Design*, pp. 385 - 388, October 1986.

[4] L. Lantz, "Soft Errors Induced by Alpha Particles", *IEEE Trans. on Reliability*, Vol. 45, pp. 174 - 179, December 1996.

[5] R. C. Baumann, "Soft Errors in Advances Semiconductor Devices-Part I: The Three Radiation Sources", *IEEE Trans. on Device and Materials Reliability*, Vol. 1, No. 1, pp. 17 – 22, 1983.

[6] R.C. Baumann, "Radiation-Induced Soft-Errors in Advanced Semiconductor Technologies", in IEEE Trans. on Device and Materials Reliability, Vol. 5, Issue 3, pp. 305-316, 2005.

[7] N. Miskov-Zivanov, D. Marculescu, "A Systematic Approach to Modeling and Analysis of Transient Faults in Logic Circuits", in Proc. of IEEE Quality of Electronic Design, (ISQED 2009), pp. 408 – 413, 2009.

[8] S. Gangadhar, M. Skoufis, S. Tragoudas, "Propagation of Transients Along Sensitizable Paths", in Proc. of IEEE Int. On-Line Testing Symposium, pp. 129 – 134, 2008.

[9] N. Seifert, B. Gill, V. Zia, M. Zhang, V. Ambrose, "On the Scalability of Redundancy Based SER Mitigation Schemes", in Proc. of IEEE Int. Integrated Circuit Design and Technology (ICICDT), pp. 1-9, 2007.

[10] T. Calin, M. Nicolaidis, R. Velazco, "Upset Hardened Memory Design for Submicron CMOS Technology", in IEEE Trans. on Nuclear Science, Vol. 43, No. 6, Dec. 1996.

[11] P. Hazucha, T. Karnik, S. Walstra, B.A. Bloechel, J.W. Tschanz, J. Maiz, K. Soumyanath, G.E. Dermer, S. Narendra, V. De, S. Borkar, "Measurements and Analysis of SER-Tolerant Latch in a 90-nm Dual-V_T CMOS Process", in *IEEE Journal of Solid-State Circuits*, Vol. 39, Issue 9, pp. 1536 – 1543, Sept. 2004.

[12] D. Rossi, M. Omaña, F. Toma, C. Metra, "Multiple Transient Faults in Logic: An Issue for Next Generation ICs?", in *Proc. of IEEE Int. Symp. on Defect and Fault tolerance in VLSI Systems*, pp. 352 - 360, 2005.

[13] M. Nicolaidis, R. Perez, D. Alexandrescu, "Low-Cost Highly-Robust Hardened Cells Using Blocking Feedback Transistors", in Proc. of IEEE VLSI Test Symposium, pp. 371 – 376, 2008.

[14] B. Gill, N. Seifert, V. Zia, "Comparison of Alpha-Particle and Neutron-Induced Combinational and Sequential Logic Error Rates at the 32nm Technology Node", in Proc. of IEEE Int. Reliability Physics Symp., pp. 199-205, 2009.

[15] S. Lin, H. Yang, R. Luo, "High Speed Soft-Error-Tolerant Latch and Flip-Flop Design for Multiple VDD Circuit", in Proc. of IEEE Computer Society Annual

[16] S. Krishnamohan, N. R. Mahapatra, "Analysis and Design of Soft-Error Hardened Latches", in Proc. of the 15th ACM Great Lakes Symposium on VLSI (GLSVLSI'05), pp. 328-331, 2005.

[17] S. Mitra, N. Seifert, M. Zhang, Q. Shi, K.S. Kim, "Robust System Design with Built-in Soft Error Resilience," IEEE Computer, Feb. 2005, pp. 43-52.

[18] M. Omaña, D. Rossi, C. Metra, "Novel Transient Fault Hardened Static Latch", in *Proc. of IEEE Int. Test Conference*, Vol. 1, pp. 886 – 892, 2003.

[19] S. Lin, Y-B. Kim, F. Lombardi, "Soft-Error Hardening Designs of Nanoscale CMOS Latches", in Proc. of IEEE VLSI Test Symp., pp. 41-46, 2009.

[20] M. Omaña, D. Rossi, C. Metra, "Latch Susceptibility to Transient Faults and New Hardening Approach", in *IEEE Transactions on Computers*, Vol. 56, Issue 9, pp. 1255 – 1268, Sep. 2007.

[21] Y. Sasaki, K. Namba, H. Ito, "Soft Error Masking Circuit and Latch Using Schmitt Trigger Circuit", in Proc. of IEEE Int. Symp. on Defect and Fault Tolerance in VLSI Systems, pp. 327-335, 2006.

[22] T. Karnik, S. Vangal, V. Veeramachaneni, P. Hazucha, V. Erraguntla, S. Borkar, "Selective Node Engineering for Chip-Level Soft Error Rate Improvement", Symp. VLSI Circuits, Dig. Tech. Papers, pp. 204 - 205, 2002.

[23] T. Monnier, F. M. Roche, J. Cosculluela, R. Velazco, "SEU Testing of a Novel Hardened Register Implemented Using Standard CMOS Technology", IEEE Trans. on Nuclear Science, Vol. 46, Issue 6, Dec. 1999.

[24] M. Omaña, D. Rossi, C. Metra, "Novel High Speed Robust Latch", in Proc. of IEEE Defect and Fault tolerance in VLSI Systems, pp. 65-73, 2009.

[25] N.A. Kurd, J.S. Barkarullah, R.O. Dizon, T.D. Fletcher, P.D. Madland, "A Multigigahertz Clocking Scheme for the Pentium® 4 Microprocessor", in IEEE Journal of Solid-State Circuits, Vol. 36, Issue 11, pp. 1647-1653, Nov. 2001.

[26] International Technology Roadmap for Semiconductors (ITRS), 2007 Edition.

[27] N.H.E. Weste, K. Eshraghian, "Principles of CMOS VLSI Design: A Systems Perspective", Addison Wesley, 1993.

[28] H. Cha and J. H. Patel, "A Logic-Level Model for α-Particle Hits in CMOS Circuits", in Proc. of IEEE Int. Conf. on Computer Design, pp. 538 – 542, 1993.

[29] P. Hazucha, C. Svensson, "Impact of CMOS Technology Scaling on the Atmospheric Neutron Soft-Error Rate", IEEE Trans. on Nuclear Science, Vol.47, No 6, Dec. 2000, pp. 2586- 2594.

Martin Omaña received the degree in Electronic Engineering from the University of Buenos Aires (Argentina) in 2000. In 2002 he was awared a MADESS grant and joined the Electronics Department of the University of Bologna, Italy, where he obtained the PhD in Electronic Engineering and Computer Science in 2005. He is currently a Post Doctoral fellow at the same University. Her research interests are in the field of design and test of digital systems, reliable and error resilient systems, fault tolerance, on-line testing, fault modeling and diagnosis and debug.

Daniele Rossi received the degree in electronic engineering and the PhD degree in electronic engineering and computer science from the University of Bologna in 2001 and 2005, respectively. His research interests include fault modeling, online testing and fault tolerance techniques, with particular focus on coding techniques for fault-tolerant and low-power buses, signal integrity for VDSM communication infrastructures, and robust design for soft error resiliency. He holds one patent. He is a member of the IEEE and the IEEE Computer Society.

Cecilia Metra is an Associate Professor in Electronics in the Department of Electronic, Computer Science and Systems (DEIS) of the Univ. of Bologna. She is also affiliated with the Advanced Research Center on Electronic Systems for Information and Communication Technologies E. De Castro (ARCES) of the Univ. of Bologna. She has been Visiting Scholar at the Univ. of Washington, Seattle (USA) from 1998 to 2001,

and Visiting Faculty Consultant for Intel Corporation, Santa Clara (CA) in 2002. She is Vice General Co-Chair of the IEEE Int'l VLSI Test Symp. 2010, and she has been General Co-Chair of The IEEE Int'l Symp. on Defect and Fault Tolerance in VLSI Systems 2005 and 1999, the IEEE Int'l On-Line Testing Symp. 2006 and the IEEE Int'l On-Line Testing Workshop 2001, and Program Chair/Co-Chair of the IEEE Int'l VLSI Test Symp. 2009 and 2008, the IEEE International Workshop on Design and Test of Nano Devices, Circuits and Systems (NDCS) 2008, The IEEE Int'l Symp. on Defect and Fault Tolerance in VLSI Systems 1998, the IEEE Int'l On-Line Testing Symp. 2005, 2004 and 2003, and the IEEE Int'l On-Line Testing Workshop 2002. She serves/served as Topic Chair and as Member of the Organizing Committee and/or Technical Program Committee of several international conferences. Her research interests are in the field of Design and Test of Integrated Digital Systems, Reliable and Error Resilient Systems, Fault Tolerance, On-Line Testing, Fault Modelling, Diagnosis and Debug, Emergent Technologies. She is Associate Editor in Chief of the IEEE Transactions on Computers, and a Member of the Editorial Board of the Journal of Electronic Testing: Theory and Applications and the International Journal of Highly Reliable Electronic System Design. She is a Golden Core member of the IEEE Computer Society.